Proceedings of the 9th World Congress on Mechanical, Chemical, and Material Engineering (MCM'23)
Brunel University, London, United Kingdom - August 06-08, 2023
Paper No. MMME 121
DOI: 10.11159/mmme23.121

Free Vibration Analysis of Porous FG Nanoplates via a New Nonlocal 2D Trigonometric High-Order Shear Deformation Theory

Mohammed Amine Kenanda[1], Fodil Hammadi[2], Zakaria Belabed[3], Youcef Abdelouahab[1]

[1] ENERGARID Laboratory, Department of Mechanical Engineering, Tahri Mohamed University, 08000 Bechar, Algeria
kenandaamine@gmail.com or kenanda.mohammedamine@univ-bechar.dz
[2] Laboratory of Mechanics, Modeling and Experimentation L2ME, Department of Mechanical Engineering, Tahri Mohamed University, 08000 Bechar, Algeria
hammadi.fodil@univ-bechar.dz
[3] Department of Technology, Institute of Science and Technology, University Ctr Naama, 45000 Naama, Algeria
belabed.zak@gmail.com
[1] ENERGARID Laboratory, Department of Mechanical Engineering, Tahri Mohamed University, 08000 Bechar, Algeria
abdelouahab.youcef@univ-bechar.dz

Abstract- In this paper, a new nonlocal two-dimensional trigonometric high-order shear deformation theory (nonlocal-2D THSDT) is developed for free vibration response of porous functionally graded nanoplates (FGNPs). There are four variables in the present displacement field, and there is no need for a shear correction factor. The mechanical properties vary continuously across the thickness of the porous FG nanoplate applying a modified power law function to account for the effect of porosity on the properties. Two new and different porosity distribution models are examined, including uniform and non-uniform porosity distributions. The nonlocal strain theory is used to consider the nanoscales, and the Navier method is used to obtain the solution of the equations of motion. A comprehensive parametric study is presented to demonstrate the influence of various parameters on the behaviour of porous FG nanoplates.

Keywords: *nonlocal elasticity theory*, *trigonometric shear deformation theory*, *FG porous nanoplates*, *uneven porosity distribution*

1. Introduction

In 1984, a team of Japanese researchers developed a new material known as functionally graded materials (FGMs) in order to achieve effective thermal insulation for spacecraft. These materials have many advantages and have been used in various fields including the space industry, mechanical and civil engineering, among others. The mechanical, thermal, and electrical properties of FGMs change continuously from the lowest material (generally metal) to the upper material (ceramic) for at least two materials.

J.N. Reddy [1] developed a simple high-order shear deformation theory, called third-order shear theory, to study the mechanical behavior of laminated plates. In recent years, many studies have been conducted to develop new high-order shear theories based on Reddy's idea, to investigate the behavior of FG structures. A.M. Zenkour [2] and M. Touratier [3] employed a new sinusoidal shear deformation theory to analyze the bending and free vibration of the FG plate and isotropic plate, respectively. According to the novel exponential function, Karama et al. [4] studied the mechanical behavior of the laminated composite plate. Kenanda et al. [5] developed a new efficient hyperbolic shear deformation theory to study the free vibration and the effect of porosities on the structural integrity of functionally graded plates. Recently, various researchers have developed new high-order shear deformation theories according to several functions, including polynomial, exponential, trigonometric, and many others, to study the behavior of FG structures. Some of them are mentioned in the references [6–12].

Shahsavari et al. [13] employed even and uneven porosity distributions to analyze the influence of porosities on the free vibration response of FG plates embedded on Kerr foundations using a simple trigonometric high-order

theory. Hygro-thermal stability analysis of porous FG panels was conducted by M. R. Barati and H. Shahverdi [14], employing even and uneven porosity distributions. Some researchers, e.g., Fu et al. [15] and Thanh et al. [16], developed new distributions based on logarithmic and trigonometric functions to study the effect of porosities on the mechanical behavior of FG plates.

The main objective of this work falls under the promotion of understanding about high-order shear deformation theories that describe the distribution of shear stresses, such as the first-order, third-order [1], sinusoidal [2], exponential [3], and hyperbolic shear deformation theories [4]. We have developed a new HSDT that is modeled by a trigonometric function that does not need a correction factor and gives more effective and accurate results compared to the 3D exact solutions.

The second objective of this research is to study the effect of porosity on structural integrity by presenting two new uneven distributions (polynomial and exponential) derived from the most famous and used distributions (even and linear-uneven) by researchers for the purpose of enriching and enhancing understanding about the effect of porosity with their different distributions.

2. Material properties

A simple supported nanoplate with uniform dimensions (thickness h, length a, and width b) that is made of imperfect functionally graded material (i.e., FGM with porosities) as shown in figure 1. The power-law function (P-FGM) serves as the foundation for the material properties of FG plate, considering the effect of porosities as follows:

- Perfect functionally graded material:

$$\Gamma(z) = (\Gamma_c - \Gamma_m)\left(\frac{z}{h} + \frac{1}{2}\right)^N + \Gamma_m \tag{1}$$

- Imperfect functionally graded material (even porosity distribution):

$$\Gamma(z) = (\Gamma_c - \Gamma_m)\left(\frac{z}{h} + \frac{1}{2}\right)^N + \Gamma_m - \frac{\beta}{2}(\Gamma_c + \Gamma_m) \tag{2}$$

- Imperfect functionally graded material (inverse-linear uneven porosity distribution):

$$\Gamma(z) = (\Gamma_c - \Gamma_m)\left(\frac{z}{h} + \frac{1}{2}\right)^N + \Gamma_m - \frac{\beta}{2}(\Gamma_c + \Gamma_m)\left(1 - \frac{2|z|}{h}\right) \tag{3}$$

Where (Γ) stands for the material characteristics, such as mass density, Young's modulus, and Poisson's ratio. (N and β) represent the power-law and porosity indexes, respectively. In this manuscript, two uneven porosity distributions are developed based on the equation 3 and can be expressed in the following form:

- Imperfect functionally graded material (inverse-cubic uneven porosity distribution):

$$\Gamma(z) = (\Gamma_c - \Gamma_m)\left(\frac{z}{h} + \frac{1}{2}\right)^N + \Gamma_m - \frac{\beta}{2}(\Gamma_c + \Gamma_m)\left(1 - \left(\frac{2|z|}{h}\right)^3\right) \tag{4}$$

- Imperfect functionally graded material (cubic uneven porosity distribution):

$$\Gamma(z) = (\Gamma_c - \Gamma_m)\left(\frac{z}{h} + \frac{1}{2}\right)^N + \Gamma_m - \frac{\beta}{2}(\Gamma_c + \Gamma_m)\left(\frac{2|z|}{h}\right)^3 \tag{5}$$

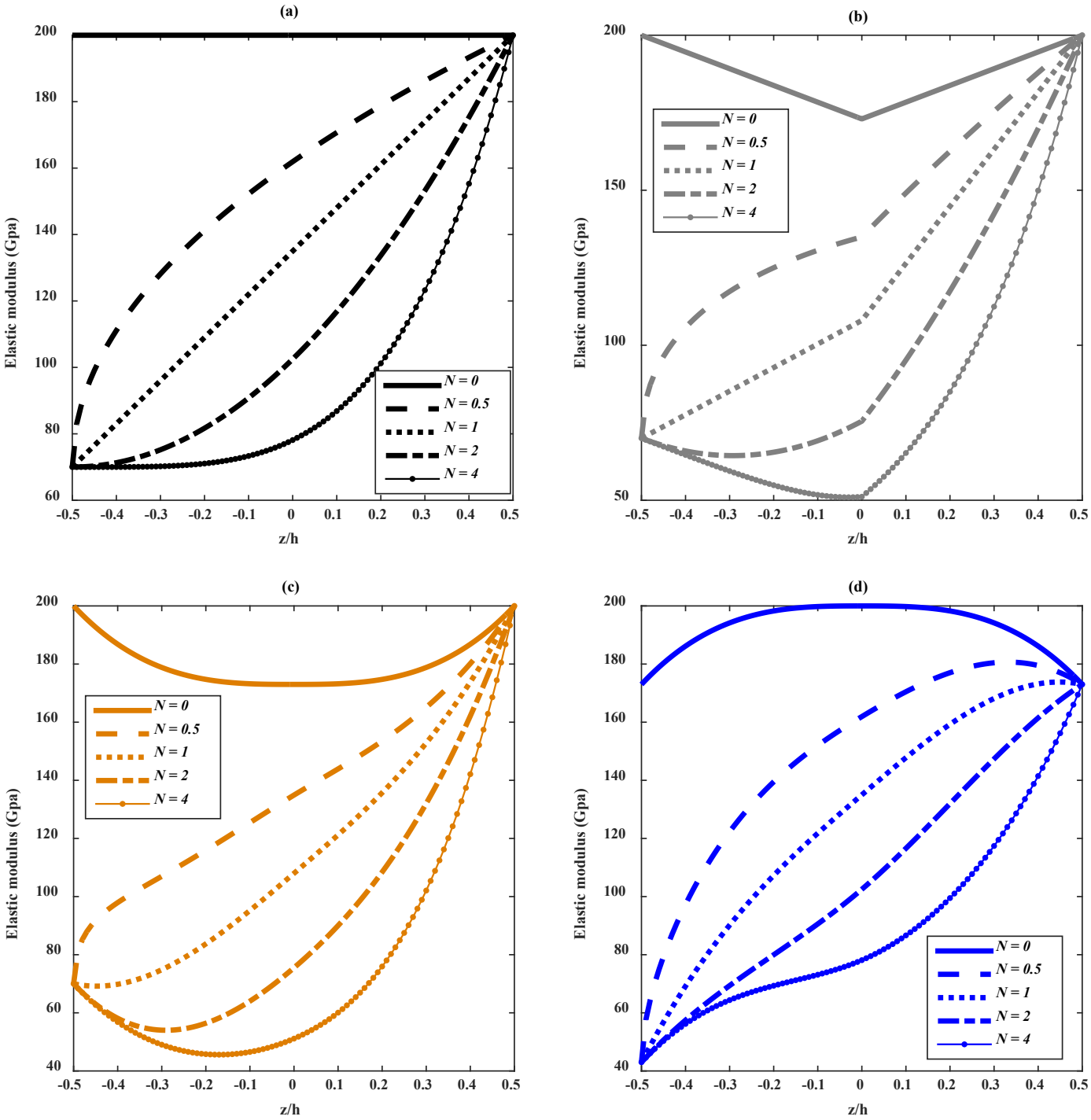

Fig. 1: The variation of the Young's modulus in terms of (z/h) for: a) perfect FGM, b) imperfect FGM (inverse-linear porosity distribution), c) imperfect FGM (inverse-cubic porosity distribution), and d) imperfect FGM (cubic porosity distribution).

3. Mathematical formulation

3.1. Displacement field and strain

The displacement field in the current analysis contains four variables (u_0, v_0, w_s, w_b) without the need for a correction factor. The present displacement field can be expressed as follows:

$$\begin{cases} u(x,y,z,t) = u_0(x,y,t) - z\frac{\partial w_b}{\partial x} - f(z)\frac{\partial w_s}{\partial x} \\ v(x,y,z,t) = v_0(x,y,t) - z\frac{\partial w_b}{\partial y} - f(z)\frac{\partial w_s}{\partial y} \\ w(x,y,z,t) = w_b(x,y,t) + w_s(x,y,t) \end{cases} \tag{6a}$$

In which

$$f(z) = z - \varphi(z) \tag{6b}$$

Where $\varphi(z)$ is the transverse shear stress distribution through the thickness. In this analysis, we propose a new high-order shear deformation theory modeled by trigonometric functions in the following forms:

$$\varphi(z) = -\frac{he^{\left(-\frac{2z}{h}\right)}\left(\left(e^{\left(\frac{4z}{h}\right)} - 10e^{\left(\frac{2z}{h}\right)} + 1\right)sin\left(\frac{z}{h}\right) + \left(2e^{\left(\frac{4z}{h}\right)} - 2\right)cos\left(\frac{z}{h}\right)\right)}{20\ cos\left(\frac{1}{2}\right)sinh^2\left(\frac{1}{2}\right)} + z \tag{6c}$$

The displacement field in Equation (6a) can be employed to calculate the strain field of a porous FG nanoplate as follows:

$$\begin{cases} \varepsilon_x = \frac{\partial u_0}{\partial x} - z\frac{\partial^2 w_b}{\partial x^2} - f(z)\frac{\partial^2 w_s}{\partial x^2} \\ \varepsilon_y = \frac{\partial v_0}{\partial y} - z\frac{\partial^2 w_b}{\partial y^2} - f(z)\frac{\partial^2 w_s}{\partial y^2} \end{cases} \tag{7a}$$

$$\begin{cases} \gamma_{xy} = \frac{\partial u_0}{\partial y} + \frac{\partial v_0}{\partial x} - 2z\frac{\partial^2 w_b}{\partial x \partial y} - 2f(z)\frac{\partial^2 w_s}{\partial x \partial y} \\ \gamma_{xz} = g(z)\frac{\partial w_s}{\partial x} \\ \gamma_{yz} = g(z)\frac{\partial w_s}{\partial y} \end{cases} \tag{7b}$$

In which

$$g(z) = 1 - \frac{df}{dz} \tag{7c}$$

To consider the effect of nano-scale dimensions of porous FG plate, the nonlocal elasticity theory [17] is used to express the linear stress–strain as:

$$\begin{Bmatrix}\sigma_x\\ \sigma_y\\ \tau_{yz}\\ \tau_{xz}\\ \tau_{xy}\end{Bmatrix} - (e_0 a)^2\left(\frac{\partial^2}{\partial x^2}+\frac{\partial^2}{\partial y^2}\right)\begin{Bmatrix}\sigma_x\\ \sigma_y\\ \tau_{yz}\\ \tau_{xz}\\ \tau_{xy}\end{Bmatrix} = \begin{bmatrix}C_{11} & C_{11} & 0 & 0 & 0\\ C_{12} & C_{12} & 0 & 0 & 0\\ 0 & 0 & C_{44} & 0 & 0\\ 0 & 0 & 0 & C_{55} & 0\\ 0 & 0 & 0 & 0 & C_{66}\end{bmatrix}\begin{Bmatrix}\varepsilon_x\\ \varepsilon_y\\ \gamma_{yz}\\ \gamma_{xz}\\ \gamma_{xy}\end{Bmatrix} \tag{8a}$$

Where (e_0 and a) are the material constant and the internal characteristic length, respectively. (C_{ij}) are the elastic constants can be obtained as depicted in equation (8b) in the case of two-dimensional analysis.

$$\begin{cases} C_{11} = C_{22} = \frac{E(z)}{(1-\nu^2)} \\ C_{12} = \frac{\nu E(z)}{(1-\nu^2)} \\ C_{44} = C_{55} = C_{66} = G(z) = \frac{E(z)}{2(1+\nu)} \end{cases} \tag{8b}$$

The equations of motion are deduced based on the Hamilton's principle (equation 9) and are solved using double Fourier series (equation 10).

$$\int_0^t (\delta E_s - \delta E_k)dt = 0 \tag{9}$$

Where (δE_s and δE_k) are the variation of the kinetic energy and strain energy, respectively.

$$\begin{Bmatrix}u_0(x,y)\\ v_0(x,y)\\ w_b(x,y)\\ w_s(x,y)\end{Bmatrix} = \sum_{m=1}^{\infty}\sum_{n=1}^{\infty}\begin{Bmatrix}U_{mn}cos(\lambda x)sin(\eta y)e^{i\omega t}\\ V_{mn}sin(\lambda x)cos(\eta y)e^{i\omega t}\\ W_{bmn}sin(\lambda x)sin(\eta y)e^{i\omega t}\\ W_{smn}sin(\lambda x)sin(\eta y)e^{i\omega t}\end{Bmatrix} \tag{10a}$$

$$\lambda = m\pi/a \quad ; \quad \eta = n\pi/b \tag{10b}$$

Where m and n are the mode numbers. Then the equations of motion are imposed in matricide form as follows:

$$\left(\begin{bmatrix}S_{11} & S_{12} & S_{13} & S_{14}\\ S_{12} & S_{22} & S_{23} & S_{24}\\ S_{13} & S_{23} & S_{33} & S_{34}\\ S_{14} & S_{24} & S_{34} & S_{44}\end{bmatrix} - \omega^2\begin{bmatrix}m_{11} & m_{12} & m_{13} & m_{14}\\ m_{12} & m_{22} & m_{23} & m_{24}\\ m_{13} & m_{23} & m_{33} & m_{34}\\ m_{14} & m_{24} & m_{34} & m_{44}\end{bmatrix}\right)\begin{Bmatrix}U_{mn}\\ V_{mn}\\ W_{bmn}\\ W_{smn}\end{Bmatrix} = \begin{Bmatrix}0\\0\\0\\0\end{Bmatrix} \tag{11a}$$

The components of the matrice S and m are expressed as follows:

$$\begin{aligned} S_{11} &= -\lambda^2(A_{11}) - \eta^2(A_{44}) \\ S_{12} &= -\eta\lambda(A_{44} + A_{12}) \\ S_{13} &= \lambda[\lambda^2(B_{11}) + \eta^2(B_{12} + 2B_{44})] \\ S_{14} &= \lambda[\lambda^2(E_{11}) + \eta^2(E_{12} + 2E_{44})] \\ S_{22} &= -\lambda^2(A_{44}) - \eta^2(A_{22}) \end{aligned}$$

$$
\begin{aligned}
S_{23} &= \eta[\eta^2(B_{22}) + \lambda^2(B_{12} + 2B_{44})] \\
S_{24} &= \eta[\eta^2(E_{22}) + \lambda^2(E_{12} + 2E_{44})] \\
S_{33} &= -[\lambda^4(D_{11}) + 2(D_{12} + 2D_{44})\lambda^2\eta^2 + \eta^4 D_{22}] \\
S_{34} &= -[\lambda^4(F_{11}) + 2(F_{12} + 2F_{44})\lambda^2\eta^2 + \eta^4 F_{22}] \\
S_{44} &= -\left[\lambda^4(G_{11}) + \left(2(G_{12} + 2G_{44})\right)\lambda^2\eta^2 + \eta^4 G_{22} + (K_{55})\lambda^2 + (K_{44})\eta^2\right]
\end{aligned} \tag{11b}
$$

$$
\begin{aligned}
m_{11} &= -D_0 L; \quad m_{12} = 0; \quad m_{13} = \lambda D_1 L; \quad m_{14} = \lambda D_2 L \\
m_{22} &= -D_0 L; \quad m_{23} = \eta D_1 L; \quad m_{24} = \eta D_2 L \\
m_{33} &= -L\left(D_0 + D_2(\lambda^2 + \eta^2)\right); \quad m_{34} = -L\left(D_0 + D_4(\lambda^2 + \eta^2)\right) \\
m_{44} &= -L\left(D_0 + D_5(\lambda^2 + \eta^2)\right) \\
L &= [1 + \mu^2(\lambda^2 + \eta^2)] \\
\mu &= e_0 a
\end{aligned} \tag{11c}
$$

The stiffness components $(A_{ij}, B_{ij}, D_{ij}, E_{ij}, F_{ij}, G_{ij}, K_{ij})$ are defined below:

$$
\begin{Bmatrix}
A_{11} & B_{11} & D_{11} & E_{11} & F_{11} & G_{11} \\
A_{22} & B_{22} & D_{22} & E_{22} & F_{22} & G_{22} \\
A_{12} & B_{12} & D_{12} & E_{12} & F_{12} & G_{12} \\
A_{44} & B_{44} & D_{44} & E_{44} & F_{44} & G_{44}
\end{Bmatrix} = \int_{-h/2}^{h/2} C_{11} \{1, z, z^2, f(z), zf(z), f^2(z)\} \begin{Bmatrix} 1 \\ 1 \\ \nu \\ \frac{1-\nu}{2} \end{Bmatrix} dz \tag{12a}
$$

$$
K_{44} = K_{55} = \int_{-h/2}^{h/2} C_{44} (g(z))^2 dz \tag{12b}
$$

$$
D_i = \int_{-h/2}^{h/2} \rho(z)(1, z, f(z), z^2, zf(z), (f(z))^2)\, dz \qquad i = 0{,}5 \tag{12c}
$$

3. Results and discussion

In this part, we devote ourselves to comparing the current exponential-trigonometric shear theory with several reference theories to prove its validity and effectiveness. Simultaneously, we aim to study the effect of porosities on the behavior of the porous FG plate. The mechanical properties used in this part are illustrated in the table1.

Table 1: The mechanical properties of the present porous functionally graded plate.

Mechanical properties	**Metal (AL)**	**Ceramic (Al_2O_3)**
$E\ (Gpa)$	70	380
ν	0.3	0.3
$\rho\ (Kg/m^3)$	2702	3800

In the table 2, the first non-dimensional frequencies for three values of the ratios a/h = 5, 10, and 20, and five values of power-law index N = 0, 0.5, 1, 4, and 10. Our results obtained by using the current HSDT are compared to the results of the first-order shear theory obtained by Hosseini-Hashemi et al. [18], high-order shear theories obtained by the references [19, 20]. The results of our current theory are largely consistent with the results of reference theories [18-20].

Moreover, we can see from the results of the Table 2 that the frequencies decrease with the increase of the power-law index *N* and the ratios a/h.

Table 2: The first non-dimensional frequencies ($\bar{\omega} = \omega h\sqrt{\rho_c/E_c}$) for various values of the ratios a/h and power-law index *N*.

a/h	Theories	Power law index *N*				
		0	0.5	1	4	10
5	FSDT [18]	0.2112	0.1805	0.1631	0.1397	0.1324
	HSDT [19]	0.2113	0.1807	0.1631	0.1378	0.1301
	HSDT [20]	0.2113	0.1807	0.1631	0.1377	0.1300
	Present	**0.2113**	**0.1807**	**0.1631**	**0.1378**	**0.1300**
10	FSDT [18]	0.0577	0.0490	0.0442	0.0382	0.0366
	HSDT [19]	0.0577	0.0490	0.0442	0.0381	0.0364
	HSDT [20]	0.0577	0.0490	0.0442	0.0381	0.0364
	Present	**0.0577**	**0.0490**	**0.0442**	**0.0381**	**0.0364**
20	FSDT [18]	0.0148	0.0125	0.0113	0.0098	0.0094
	HSDT [19]	0.0148	0.0125	0.0113	0.0098	0.0094
	HSDT [20]	0.0148	0.0125	0.0113	0.0098	0.0094
	Present	**0.0148**	**0.0125**	**0.0113**	**0.0098**	**0.0094**

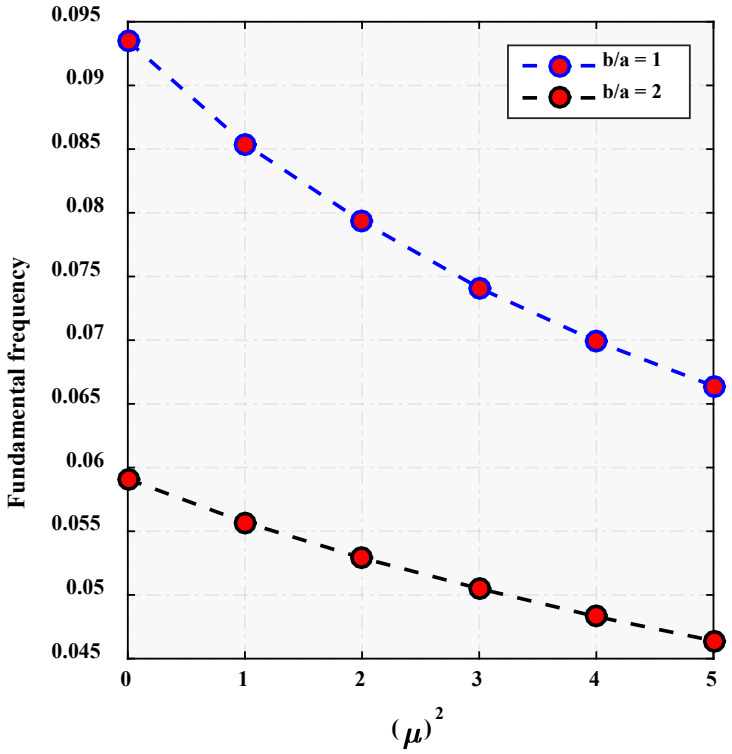

Fig. 2: The effect of nano-scales (μ^2) on the non-dimensional frequencies ($\tilde{\omega} = \omega h\sqrt{\rho/G}$) of square and rectangular isotropic nano-plates.

Table 3: The effect of porosities on the non-dimensional frequencies ($\bar{\omega} = \omega h\sqrt{\rho_c/E_c}$) of FG plates for three uneven porosity distributions (inverse-linear, inverse-cubic, and cubic) at (a/h = 10, $N = 2$, and $\mu^2 = 0$).

Uneven Porosity Distribution	**Porosity index β**		
	$\beta = 0$	$\beta = 0.2$	$\beta = 0.4$
Inverse-linear UPD	0.04009	0.03961	0.03858
Inverse-cubic UPD	0.04009	0.03836	0.03413
cubic UPD	0.04009	0.37574	0.34404

The figure 2 presents the effect of nano-scales (μ^2) on the non-dimensional frequencies ($\widetilde{\omega} = \omega h\sqrt{\rho/G}$) of square and rectangular isotropic nano-plates. It is noted from Figure 2 that an increase in the value of μ^2 leads to a decrease in frequencies, and the frequencies of the square FG plate are greater than those of the rectangular FG plate. The effect of the three porosity distributions on the frequencies is clear in Table 3, where the porosities lead to a decrease in frequencies for all distributions.

4. Conclusion

The present theory describes the distribution of shear stress by employing a novel exponential-trigonometric function that eliminates the need for a shear correction factor. This theory also satisfies the zero traction boundary conditions on both the top and bottom surfaces of the porous FG nano-plate. The displacement field of the 2D exponential-trigonometric shear deformation theory encompasses only four variables. In comparison to other shear deformation theories, the proposed hyperbolic theory is more comprehensive and accurately represents the transverse shear stress. Consequently, it yields superior results in describing the mechanical behavior of FG plates. Furthermore, the current exponential-trigonometric function can be employed as a refined theory without any modifications. This is attributed to its segmented form, similar to the third-order shear deformation theory. The eigenvalue problem of the advanced shear deformation theory is solved using Navier's solution approach.

References

[1] J. N. Reddy, "Analysis of functionally graded plates," *International Journal for numerical methods in engineering*, vol. 47, no 1-3, pp. 663-684, 2000.

[2] A. M. Zenkour, "Generalized shear deformation theory for bending analysis of functionally graded plates," *Applied Mathematical Modelling*, vol. 30, no 1, p. 67-84, 2006.

[3] M. Touratier, "An efficient standard plate theory," *International journal of engineering science*, vol. 29, no 8, pp. 901-916, 1991.

[4] M. Karama, K. S. Afaq, S. Mistou, "A new theory for laminated composite plates," *Proceedings of the Institution of Mechanical Engineers, Part L: Journal of Materials: Design and Applications*, vol. 223, no 2, pp. 53-62, 2009.

[5] M. H. Meliani, M. A. Kenanda, F. Hammadi, Z. Belabed, "Free vibration analysis of the structural integrity on the porous functionally graded plates using a novel Quasi-3D hyperbolic high order shear deformation theory," *Frattura ed Integrità Strutturale*, vol. 17, no 64, pp. 266-282, 2023.

[6] S. S. Akavcik, A. H. Tanrikulu, "Static and free vibration analysis of functionally graded plates based on a new quasi-3D and 2D shear deformation theories," *Composites Part B: Engineering*, vol. 83, p. 203-215, 2015.

[7] S. S. Akavci, "An efficient shear deformation theory for free vibration of functionally graded thick rectangular plates on elastic foundation," *Composite Structures*, vol. 108, p. 667-676, 2014.

[8] Z. Belabed, M. S. A. Houari, A. Tounsi, S. R. Mahmoud, O. A. Bég, "An efficient and simple higher order shear and normal deformation theory for functionally graded material (FGM) plates," *Composites Part B: Engineering*, vol. 60, p. 274-283, 2014.

[9] M. Li, C. G. Soares, R. Yan, "novel shear deformation theory for static analysis of functionally graded plates," *Composite Structures*, vol. 250, p. 112559, 2020.

[10] M. Li, C. G. Soares, R. Yan, “Free vibration analysis of FGM plates on Winkler/Pasternak/Kerr foundation by using a simple quasi-3D HSDT,” *Composite Structures*, vol. 264, p. 113643, 2021.
[11] M. Malikan, V. A. Eremeyev, “A new hyperbolic-polynomial higher-order elasticity theory for mechanics of thick FGM beams with imperfection in the material composition,” *Composite Structures*, vol. 249, p. 112486, 2020.
[12] F. Z. Zaoui, D. Ouinas, A. Tounsi, “New 2D and quasi-3D shear deformation theories for free vibration of functionally graded plates on elastic foundations,” *Composites Part B: Engineering*, vol. 159, p. 231-247, 2019.
[13] D. Shahsavari, M. Shahsavari, L. Li, B. Karami, “A novel quasi-3D hyperbolic theory for free vibration of FG plates with porosities resting on Winkler/Pasternak/Kerr foundation,” *Aerospace Science and Technology*, vol. 72, p. 134-149, 2018.
[14] M. R. Barati, H. Shahverdi, “Aero-hygro-thermal stability analysis of higher-order refined supersonic FGM panels with even and uneven porosity distributions,” *Journal of Fluids and Structures*, vol. 73, p. 125-136, 2017.
[15] T. Fu, X. Wu, Z. Xiao, Z. Chen, “Thermoacoustic response of porous FGM cylindrical shell surround by elastic foundation subjected to nonlinear thermal loading,” *Thin-Walled Structures*, vol. 156, p. 106996, 2020.
[16] C. L. Thanh, L. V. Tran, T. Q. Bui, H. X. Nguyen, M. Abdel-Wahab, “Isogeometric analysis for size-dependent nonlinear thermal stability of porous FG microplates,” *Composite Structures*, vol. 221, p. 110838, 2019.
[17] A. C. Eringen, D. Edelen, “On nonlocal elasticity,” International journal of engineering science, vol. 10, no 3, p. 233-248, 1972.
[18] S. Hosseini-Hashemi, M. Fadaee, S. R. Atashipour, “A new exact analytical approach for free vibration of Reissner–Mindlin functionally graded rectangular plates,” International Journal of Mechanical Sciences, vol. 53, no 1, p. 11-22, 2011.
[19] S. Hosseini-Hashemi, M. Fadaee, S. R. Atashipour, “Study on the free vibration of thick functionally graded rectangular plates according to a new exact closed-form procedure,” Composite Structures, vol. 93, no 2, p. 722-735, 2011.
[20] H. T. Thai, T. P. Vo, “A new sinusoidal shear deformation theory for bending, buckling, and vibration of functionally graded plates,” Applied mathematical modelling, vol. 37, no 5, p. 3269-3281, 2013.